Rapidity Dependence of Charged Antihadron to Hadron Ratios in Au + Au Collisions at $\sqrt{s_{NN}} = 200$ GeV

I. G. Bearden,[7] D. Beavis,[1] C. Besliu,[10] Y. Blyakhman,[6] B. Budick,[6] H. Bøggild,[7] C. Chasman,[1] C. H. Christensen,[7] P. Christiansen,[7] J. Cibor,[3] R. Debbe,[1] E. Enger,[12] J. J. Gaardhøje,[7] M. Germinario,[7] K. Hagel,[8] O. Hansen,[7] A. Holm,[7] A. K. Holme,[12] H. Ito,[11] E. Jakobsen,[7] A. Jipa,[10] F. Jundt,[2] J. I. Jørdre,[9] C. E. Jørgensen,[7] R. Karabowicz,[4] T. Keutgen,[8] E. J. Kim,[1] T. Kozik,[4] T. M. Larsen,[12] J. H. Lee,[1] Y. K. Lee,[5] G. Løvhøiden,[12] Z. Majka,[4] A. Makeev,[8] B. McBreen,[1] M. Mikelsen,[12] M. Murray,[8] J. Natowitz,[8] B. S. Nielsen,[7] J. Norris,[11] K. Olchanski,[1] J. Olness,[1] D. Ouerdane,[7] R. Płaneta,[4] F. Rami,[2] C. Ristea,[10] D. Röhrich,[9] B. H. Samset,[12] D. Sandberg,[7] S. J. Sanders,[11] R. A. Scheetz,[1] P. Staszel,[7] T. S. Tveter,[12] F. Videbæk,[1] R. Wada,[8] A. Wieloch,[4] Z. Yin,[9] and I. S. Zgura[10]

(BRAHMS Collaboration)

[1]*Brookhaven National Laboratory, Upton, New York 11973*
[2]*Institut de Recherches Subatomiques and Université Louis Pasteur, Strasbourg, France*
[3]*Institute of Nuclear Physics, Krakow, Poland*
[4]*Smoluchkowski Institute of Physics, Jagiellonian University, Krakow, Poland*
[5]*Johns Hopkins University, Baltimore, Maryland 21218*
[6]*New York University, New York, New York 10003*
[7]*Niels Bohr Institute, Blegdamsvej 17, University of Copenhagen, Copenhagen 2100, Denmark*
[8]*Texas A&M University, College Station, Texas 17843*
[9]*Department of Physics, University of Bergen, Bergen, Norway*
[10]*University of Bucharest, Romania*
[11]*University of Kansas, Lawrence, Kansas 66049*
[12]*Department of Physics, University of Oslo, Oslo, Norway*

(Received 12 July 2002; published 12 March 2003)

We present ratios of the numbers of charged antihadrons to hadrons (pions, kaons, and protons) in Au + Au collisions at $\sqrt{s_{NN}} = 200$ GeV as a function of rapidity in the range $y = 0$–3. While the ratios at midrapidity are approaching unity, the K^-/K^+ and $\bar{p}/p$ ratios decrease significantly at forward rapidities. An interpretation of the results within the statistical model indicates a reduction of the baryon chemical potential from $\mu_B \approx 130$ MeV at $y = 3$ to $\mu_B \approx 25$ MeV at $y = 0$.

DOI: 10.1103/PhysRevLett.90.102301 PACS numbers: 25.75.Dw

Ratios of yields of antihadrons to hadrons and, in particular, the rapidity dependence of such ratios are significant indicators of the dynamics of high energy nucleus-nucleus collisions [1,2]. At the energy of $\sqrt{s_{NN}} =$ 200 GeV, considerable reaction transparency is expected for Au + Au collisions, even for central events. This should lead to a flat multiplicity density as a function of rapidity (y) near midrapidity and to $\bar{p}/p$ and K^-/K^+ particle yield ratios with values near unity. Away from midrapidity the net baryon content originating from the initial nuclei is significant and production mechanisms other than particle-antiparticle pair production play a substantial role. Therefore, $\bar{p}/p$ and K^-/K^+ ratios will decrease with increasing rapidity $|y|$. Measurements of $\bar{p}/p$ ratios at 130 GeV [3–6] and of pseudorapidity distributions of charged particles at 130 [7] and 200 GeV [8,9] point to the development described above, reminiscent of the Bjorken picture [10]. Furthermore, the ratios of hadrons measured at AGS and SPS energies can be explained by assuming that the emitting source is in chemical and thermal equilibrium. This also appears to be the case [11] at $y \approx 0$ for Au + Au collisions at $\sqrt{s_{NN}} =$ 130 GeV. It is a challenge to explore this assumption at the maximum energy available in the center of mass and, in particular, as a function of rapidity, thereby scanning the particle source properties along its longitudinal extent from the central net baryon poor zone to the baryon rich region closer to fragment rapidities.

In this Letter, we present the first measurements of the ratios π^-/π^+, K^-/K^+, and $\bar{p}/p$ as a function of rapidity, transverse momentum (p_T), and collision centrality (top 20%) for Au + Au collisions at $\sqrt{s_{NN}} = 200$ GeV.

The data were obtained with the BRAHMS detector, which consists of two independent small-aperture magnetic spectrometers that can rotate in the horizontal plane about the nominal interaction point (IP). The detector covers the rapidity range $-0.1 < y < 4$ for pions and $-0.1 < y < 3.4$ for protons [12]. The MidRapidity Spectrometer (MRS) consists of two time projection chambers (TPC) and a magnet, for determining particle momenta. This assembly is followed by a segmented scintillator time-of-flight (TOF) wall, with time resolution $\sigma_t \approx 75$ ps, for velocity measurements. Requiring a $\pm 2\sigma_t$ cut around the expected flight time, $\pi - K$

separation is achieved up to a momentum of 2.3 GeV/c and $K-p$ separation up to 3.9 GeV/c. The Front Forward Spectrometer consists, in order, of a dipole magnet, a TPC, a second dipole magnet, a second TPC, a time-of-flight wall (TOF1), and a threshold gas-Cherenkov detector (C1). At small polar angles (from 2.3° to 15°), where the mean momentum of particles is large, a back section with two dipole magnets, three drift chambers, a time-of-flight wall (TOF2), and a ring imaging Cherenkov detector (RICH) is also used. TOF1 (at 8.6 m) and TOF2 (at 18 m) allow for $K-p$ separation up to $p = 5.5$ and 8 GeV/c, respectively. C1 identifies pions in the range from $p = 3$ to 9 GeV/c, and the RICH allows $\pi - K$ separation up to $p = 25$ GeV/c and $K-p$ separation from $p = 10$ to 35 GeV/c.

The reaction centrality was determined using a plastic scintillator tile array surrounding the intersection region [7,8,12]. Beam-beam counters (BBC) consisting of two arrays of Cherenkov radiators positioned ± 2.15 m from the IP were used to measure charged hadrons in the pseudorapidity range $3.0 < |\eta| < 3.8$. For the 25% most central collisions, the BBCs allow collision vertex determination with resolution $\sigma_z \approx 0.65$ cm and supply the start time for the flight time measurements with $\sigma_t \lesssim 30$ ps.

The data presented here were collected with the MRS at 40°, 60°, and 90° and the FS at 4°, 8°, 12°, and 20°. For magnetic fields of the same magnitude but opposite polarities, the spectrometer acceptance is identical for positive and negative particles. Therefore, most systematic errors associated with acceptance and detector efficiency cancel in the particle ratios. In general, the experimental methods employed here are the same as those described in Ref. [3].

Figure 1 shows the particle identification capability. The number of particles measured in various runs $[\langle d^2n/dp_T dy\rangle \Delta p_T \Delta y]$ is normalized to the number of collision events fulfilling a given centrality cut. The geometrical acceptances of the spectrometers change as a function of the collision vertex and the normalization is done depending on the collision vertex, thus accounting for possible differences in the vertex distributions from run to run. From the normalized number of antiparticles and particles the ratios are calculated.

The ratios have been corrected for absorption and production of secondary particles in the material traversed (Be beam tube, various detector elements, and air). Losses of antiprotons due to annihilation have been evaluated in GEANT simulations to be about 3% in the MRS and 0.9% in the FS. In the MRS the background contribution to proton yields, arising mainly from the interaction of pions with the beam tube, is $\approx 10\%$ for the lowest p_T bin at midrapidity falling off to 2% at $p_T > 0.5$ GeV. In the FS this contribution is found to be less than 1% at 30° and negligible at smaller angles. For kaons decay losses cancel out, and

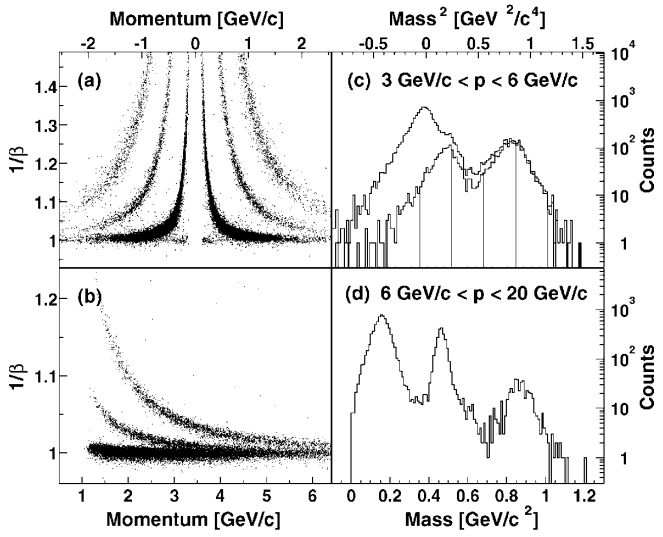

FIG. 1. Particle identification capability in BRAHMS. (a),(b) Separation between pions, kaons, and protons. The MRS (a) is at 90° and both charges are accepted. The FS (b) is here positioned at 12°. (c) Mass-squared spectrum in the FS from time-of-flight measurements. The shaded histogram includes the vetoing of pions in C1. (d) Mass spectrum in FS using the RICH.

differences in reaction cross sections for K^- and K^+ amount to less than 1%.

Figure 2 shows the dependence of the ratios for pions, kaons, and protons (corrected as described above) on transverse momentum p_T [2(a) and 2(c)] and collision centrality [2(b) and 2(d)] in two selected rapidity intervals, around $y = 0$ and $y \approx 2$, respectively. The measured ratios show no significant dependence on p_T or centrality in the covered ranges. Therefore, we integrate our yields over the centrality range 0%–20% and the p_t within our acceptance before calculating the ratios.

The ratios shown in Fig. 2 have not been corrected for protons and antiprotons that originate from weak decays of hyperons (Λ, Σ, etc.). Corrections for feed down depend on the relative production of hyperons and primary baryons and their antiparticles and on the respective spectrum slopes. PHENIX has determined $\Lambda/p = 0.89 \pm 0.07 \pm 0.21$ and $\bar{\Lambda}/\bar{p} = 0.95 \pm 0.09 \pm 0.22$ (after Λ feed down correction), and STAR has measured (no feed down correction) $\bar{\Lambda}/\Lambda = 0.74 \pm 0.04$ at $y = 0$ for $\sqrt{s_{NN}} = 130$ GeV collisions [13]. We have studied the magnitude of the corrections using various model assumptions as input to realistic GEANT simulations of the BRAHMS setup. Assuming primary hyperon/baryon ratios similar to those measured at $y = 0$ [13], we find that the corrections to the quoted ratios in our acceptance are less than 5%.

Figure 3 shows the π^-/π^+, K^-/K^+, and $\bar{p}/p$ ratios as a function of rapidity. Systematic uncertainties are estimated as 4% primarily from differences in normalizations at opposite polarity settings. While the π^-/π^+ ratio

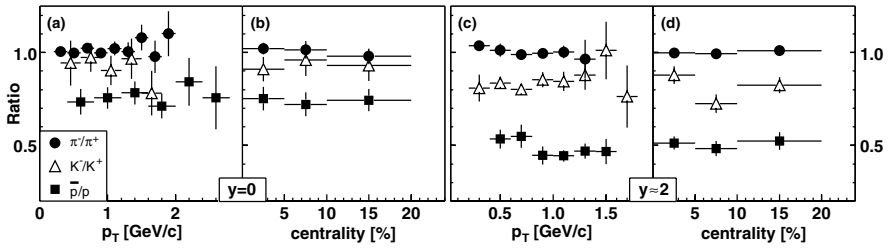

FIG. 2. Dependence of the measured antihadron to hadron ratios on p_T and reaction centrality. Panels (a) and (b) are for $y = 0$ and panels (c) and (d) for rapidities in the range $y = 2.05$ for protons to $y = 2.55$ for pions. Errors are statistical.

is consistent with unity over the considered rapidity range, the K^-/K^+ ratio shows a decrease from 0.95 ± 0.05, at $y = 0$, to 0.67 ± 0.06, at $y = 3.05$. Likewise, the $\bar{p}/p$ ratio decreases from 0.75 ± 0.04, at $y = 0$, to 0.23 ± 0.03, at $y = 3.1$. Recent PHOBOS measurements [14] at $y = 0$ agree with the measurements presented here. The $\bar{p}/p$ ratio at $y = 0$ exceeds the ratio measured in Au + Au collisions at 130 GeV [3–5] by about 17%. We also note that the $\bar{p}/p$ and K^-/K^+ ratios are essentially constant in the rapidity interval $y = 0$–1.

The measured set of particle ratios at midrapidity lends itself to an analysis in terms of a model based on the assumption of a system in chemical and thermal equilibrium such as has already been advocated for nuclear collisions at SPS energies and for elementary collisions. All yield ratios can be fitted by two parameters, the temperature T and the baryon chemical potential μ_B, and by enforcing conservation laws. Figure 4 shows the correlation between the kaon and proton ratios and a comparison to calculations with the statistical model. Our K^-/K^+ and $\bar{p}/p$ ratios are measured at slightly different rapidities. Therefore, the kaon ratios in Fig. 4 are interpolated to the y value of the proton measurements. Recently, particle ratios measured at $\sqrt{s_{NN}} =$ 130 GeV in the midrapidity region have been analyzed in a grand canonical ensemble with baryon number, strangeness, and charge conservation [11]. Values of $T = 174 \pm 7$ MeV and $\mu_B = 46 \pm 5$ MeV were found. In Ref. [11] a parametrization as a function of energy is proposed, leading to a prediction for $\sqrt{s_{NN}} = 200$ GeV of $T = 177 \pm 7$ MeV, $\mu_B = 29 \pm 8$ MeV, and, thus, $\bar{p}/p = 0.752$, $K^-/K^+ = 0.932$, and $\pi^-/\pi^+ = 1.004$. We note the excellent numerical agreement between these calculations and the present measurements. Within such an approach, the near constancy of the temperature for chemical freezeout found at SPS, at lower RHIC energies, and at the present energy can be thought of as associated with a fixed deconfinement transition temperature and the establishment of chemical equilibrium

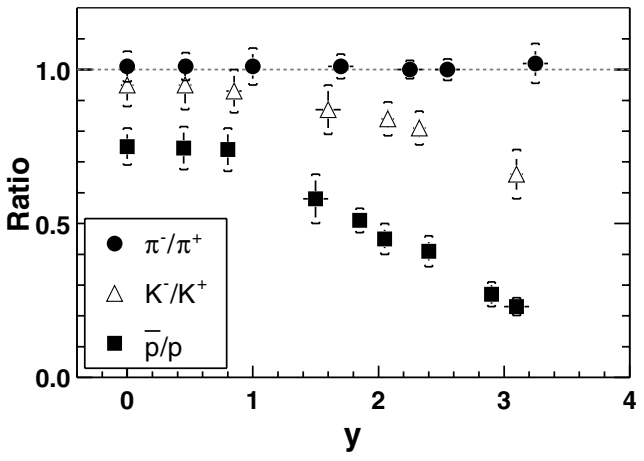

FIG. 3. Antihadron to hadron ratios as a function of rapidity. Error bars show the statistical errors while the caps indicate the combined statistical and systematic errors.

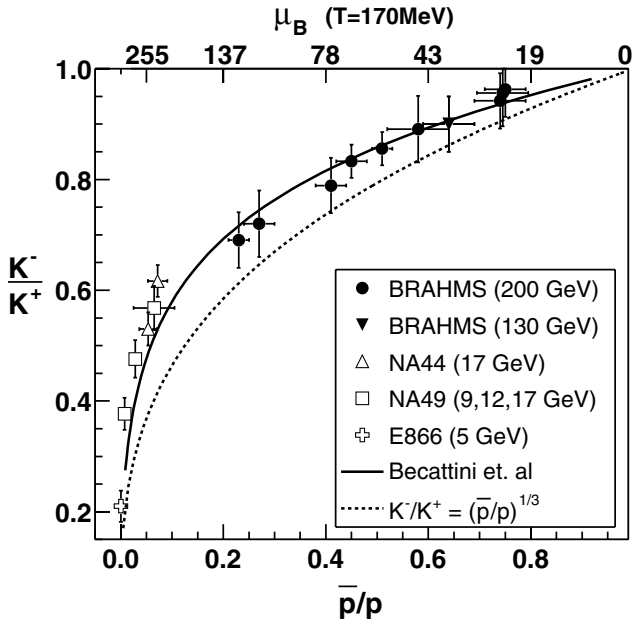

FIG. 4. Correlation between kaon and baryon ratios. Solid symbols: present work and data from Ref. [3]. The open symbols show lower energy data [15–17] at the listed center of mass energies. The line shows the statistical model prediction of Becattini *et al.* [18]. The top scale for the baryon chemical potential μ_B is in MeV. Error bars represent statistical and systematics errors.

during hadronization. The small value of the chemical potential indicates a small net baryon density at midrapidity.

A particularly interesting scenario is the breakup of a quark-gluon plasma and its subsequent hadronization. In that case, conservation of strangeness at the quark level and at the hadron level leads to the relation $\mu_S = 1/3\mu_B$, where S denotes a strange meson. The ratios of particle to antiparticle are given by quark recombination: simple quark counting gives $\bar{p}/p = \exp(-6\mu_q/T)$ and $K^-/K^+ = \exp(-2\mu_q/T) \times \exp(+2\mu_s/T)$, where q and s stand for light and strange quarks, respectively. In the hadron gas the relationship between μ_S and μ_B depends on the temperature. The 1/3 proportionality is approached only for $T = 190$ MeV and $\mu_B < 500$ MeV [19,20]. The dependence of the kaon ratio on μ_B has been predicted within such a hadron gas model [21]: K^-/K^+ decreases monotonically from 1 at $\mu_B = 0$ to 0.78 at $\mu_B = 0.1$ GeV and 0.47 at $\mu_B = 0.34$ GeV. It is remarkable that the measured K^-/K^+ vs $\bar{p}/p$ ratios measured at RHIC energies at different rapidities (Fig. 4) follow the expected relationship between the strange and baryon chemical potentials and connects to the dependence measured around midrapidity at lower energies.

Also shown are similar ratios determined at AGS [15] and SPS energies [16,17]. The correlation between the ratios at RHIC energies can be expressed as a power law $K^-/K^+ = (\bar{p}/p)^\alpha$ with $\alpha = 0.24 \pm 0.02$ and follows well the statistical model prediction [18] for a hadron gas at a constant temperature of 170 MeV. However, the lower energy data ($\alpha = 0.20 \pm 0.01$) lie slightly above. Caution must be exercised in interpreting the observed relationship as a proof of equilibration since the data points are from narrow rapidity intervals, around midrapidity at SPS and in the range $y = 0$–3 at RHIC. Within the framework of the statistical model, Fig. 4 suggests that the baryon chemical potential decreases from $\mu_B \approx 130$ MeV at $y \approx 3$ to $\mu_B \approx 25$ MeV at $y = 0$, if the temperature is assumed to be constant.

In summary, the BRAHMS experiment has measured the ratios of charged hadrons at the RHIC top energy and observed the highest such ratios yet in nuclear collisions. We find an increase in the ratio of antiprotons to protons and negative to positive kaons, consistent with a significant increase in reaction transparency compared to lower energies. The ratios are, within errors, constant in the interval $y = 0$–1 as expected for a boost invariant midrapidity plateau dominated by particle production from the color field. The ratios are well reproduced by statistical model calculations in which the baryon chemical potential decreases strongly from forward rapidities, where the baryon content of the original colliding nuclei is still significant, towards midrapidity. The systematics of kaon and proton ratios demonstrates a strongly correlated relationship between light and strange quark chemical potentials.

This work was supported by the division of Nuclear Physics of the Office of Science of the U.S. DOE, the Danish Natural Science Research Council, the Research Council of Norway, the Polish State Committee for Scientific Research, and the Romanian Ministry of Research. We are indebted to F. Becattini for supplying us with thermal model calculations.

[1] N. Hermann *et al.*, Annu. Rev. Nucl. Part. Sci. **49**, 581 (1999).
[2] H. Satz, Rep. Prog. Phys. **63**, 1511 (2000).
[3] BRAHMS Collaboration, I. G. Bearden *et al.*, Phys. Rev. Lett. **87**, 112305 (2001).
[4] STAR Collaboration, C. Adler *et al.*, Phys. Rev. Lett. **86**, 4778 (2001).
[5] PHOBOS Collaboration, B. B. Back *et al.*, Phys. Rev. Lett. **87**, 102301 (2001).
[6] PHENIX Collaboration, W. A. Zajc *et al.*, Nucl. Phys. **A698**, 39c (2002).
[7] BRAHMS Collaboration, I. G. Bearden *et al.*, Phys. Lett. B **523**, 227 (2001).
[8] BRAHMS Collaboration, I. G. Bearden *et al.*, Phys. Rev. Lett. **88**, 202301 (2002).
[9] PHOBOS Collaboration, B. B. Back *et al.*, Phys. Rev. Lett. **88**, 022302 (2002).
[10] J. D. Bjorken, Phys. Rev. D **27**, 140 (1983).
[11] P. Braun-Munzinger *et al.*, Phys. Lett. B **518**, 41 (2001).
[12] BRAHMS Collaboration, M. Adamczyk *et al.*, Nucl. Instrum. Methods (to be published).
[13] STAR Collaboration, C. Adler *et al.*, Phys. Rev. Lett. **89**, 092301 (2002); PHENIX Collaboration, K. Adcox *et al.*, *ibid.* **89**, 092302 (2002).
[14] PHOBOS Collaboration, B. B. Back *et al.*, nucl-ex/0206012.
[15] E866 Collaboration, L. Ahle *et al.*, Phys. Rev. Lett. **81**, 2650 (1998); Phys. Rev. C **60**, 044904 (1999).
[16] NA49 Collaboration, S.V. Afanasiev *et al.*, nucl-ex/0205002; nucl-ex/0208014; M. Van Leeuven, nucl-ex/020814; P. Seyboth (private communication).
[17] NA44 Collaboration, I. G. Bearden *et al.*, Phys. Rev. C **66**, 044907 (2002).
[18] F. Becattini *et al.*, Phys. Rev. C **64**, 024901 (2001); (private communication).
[19] P. Koch *et al.*, Phys. Rep. **142**, 167 (1986).
[20] J. Cleymans and H. Satz, Z. Phys. C **57**, 135 (1993).
[21] K. Redlich *et al.*, Nucl. Phys. **A566**, 391 (1994).